Article Type: Research

OPEN ACCESS

Seismic response analysis of tunnels using a coupled polygonal finite element method

Vida Nikvand[1], Masoud Hajialilue Bonab[1,*]

[1]Department of Civil Engineering, University of Tabriz, Tabriz 5166616471, Iran
*Corresponding author: hajialilue@tabrizu.ac.ir

Received: 10 July 2024 / Accepted: 22 July 2024 / Published: 25 August 2024

***Abstract*:** Mesh generation in the pre-processing stage of a conventional finite element analysis, can be a time-consuming procedure. Different methods have been proposed to modify this drawback. One of the proposed methods is the polygonal finite element technology. The polygonal finite element method (PFEM) enhances the conventional finite element (FE) approach with two major modifications. First, using polygonal elements causes mesh generation significantly easier. Second, by incorporation of more nodes per element, interpolation can be done more precisely. Like the conventional finite element method (FEM), the PFEM cannot model solely radiation damping effect of an unbounded media. In this paper, for the first time, the PFEM is coupled with the scaled boundary finite element method (SBFEM) and the proposed method is employed to evaluate seismic soil-structure interaction problems. Two shaking table tests are designed and used to model seismic tunnel responses. Then by using the achieved experimental results, accuracy and efficiency of the PFEM-SBFEM are investigated. It is shown that the introduced numerical approach leads to results that are in excellent agreement with those of the designed shaking table tests.

Keywords: Scaled boundary method; Polygonal finite element method; Tunnel; Seismic analysis; Shaking table.

I. INTRODUCTION

Numerical approaches have been widely known as an attractive and efficient procedure for solving complex geo-structure boundary value problems (BVPs). There are lots of methods that can be applied to analyze these problems. For example, the finite differences method, FDM (Hajialilue-Bonab et al., 2015; Razavi et al., 2017), the finite element method, FEM (Nath et al., 2013; Zhou et al., 2014), meshless approaches (Chen et al., 1998; Binesh et al., 2014), the discrete element method, DEM (Bretas et al., 2016; Xu & Ye, 2019) and the boundary element procedures (Grigoriev et al., 2004a,b) have been employed successfully to evaluate BVPs previously. In the use of most of these methods, a predefined mesh or at least a predefined integration cell is required. Creating a mesh for different problems, especially with complex geometry, can be a time-consuming task in the preprocessing stage of an analysis.

The polygonal finite element method (PFEM) is a feasible approach in both the pre-processing and processing stages of an analysis (Sukumar et al., 2004). The PFEM has been applied in solving diverse problems. Sukumar & Tabarraei (2004) developed a conforming PFEM to analyze problems of solid mechanics. Tabarraei & Sukumar (2006) used the PFEM for nonlinear analysis. Biabanaki & Khoei (2012) applied a PFEM to model large deformation problems. Talischi et al. (2014) used the PFEM to model incompressible fluid flow. Chi et al. (2015) proposed a PFEM to model finite elasticity problems. Nguyen-Xuan et al. (2017a) present a novel adaptive PFEM to analyze cracked structures. Nguyen-Xuan (2017b) used the presented adaptive PFEM for topology optimization in another research. The polygonal finite element method was applied to analyze plates by Nguyen-Xuan (2017c), as well. Rajagopal et al. (2018) used the PFEM to model hyperelastic material behavior.

As the reviewed literature indicates, the polygonal finite element method is rarely applied for seismic problems. Same with the conventional finite element method, the pure PFEM cannot model the radiation damping effect accurately. A usual way to model wave propagation problems is the application of boundary discretizing approaches. The conventional boundary element method (BEM) is a strong technology which can be employed to model geo-structural boundary value problems. Seepage (Rafiezadeh et al., 2014), static (Ribeiro et al., 2014) and dynamic problems (Pak et al., 1999) have been successfully analyzed so far by the boundary element method. A fundamental solution is required in the boundary element modeling of different problems. The fundamental solution is an exact answer for governing differential equation and should satisfy the governed partial differential equation (PDE) in the whole of the domain. Calculating this fundamental solution for different problems can lead to many computational efforts and make the BEM computationally expensive.

An alternative semi-analytical method to model seismic problems is the perfectly matched layer (PML). The perfectly matched layer method acts as an absorbing layer that can almost

completely avoid reflection of waves from a boundary of problem. So, the PML can model the radiation damping effect accurately. The PML was presented by Berenger (1994) for electromagnetic problems, firstly. For elasto-dynamic wave propagation problems, Chew & Liu (1996) presented the modified PML formulation. The PML method can be coupled with the FEM or other numerical approaches. For example, Fontara et al. (2017) applied the coupled PML-FEM to solve dynamic and seismic soil-structure interaction problems and Duan et al. (2016) used the PML for computing the eigenmodes of elastic waves in buried pipelines.

The infinite element method (IFEM) is another numerical approach to model wave propagation problems in unbounded domains. The coupled IFEM-FEM is used frequently to model wave propagation problems in semi-infinite unbounded domains. These efforts indicate that the infinite element method can be employed to model the radiation damping effect satisfactorily (Yeong-bin et al., 2009). Yang et al. (2003) and Yang and Hung (1997) used the FE-IFE method to model train induced vibration and its effect on adjacent structures.

In recent years, Wolf & Song (1996) developed a novel boundary discretization approach that does not require any fundamental solution. This method, which is called scaled boundary method, is a semi-analytical approach and couples the main advantages of the two FEM and BEM (Deeks et al., 2002). In the scaled boundary method (SBM), a scaling center (SC) and two dimensionless local coordinates (η, ξ), for two-dimensional (2D) problems, should be defined to transform the governing equations to the scaled boundary coordinate system. The schematic domain discretization approach in the scaled boundary method can be detailed as shown in Figure 1. Same as the BEM, the SBM has been applied to solve various engineering problems. For example, the SBM has been employed to model seepage (Bazyar et al., 2015), static (Lin et al., 2014) and dynamic problems (Hajialilue-Bonab et al., 2015; Hajialilue-Bonab & Tohidvand, 2015).

To model seismic soil-structure interaction (SSSI) problems, Junyi et al. (2003) used a free field input model based on the coupled scaled boundary finite element-finite element (SBFE-FE) method in the time domain. Genes and Kocak (2002) used the SBFE-FE method to evaluate seismic soil-structure interaction problems. A nonlinear seismic analysis was carried out in Celebi et al. (2012) to predict building responses to earthquake loading. Seiphoori et al. (2011) used the SBFE-FE method for three-dimensional analysis of concrete rockfill dams. Bazyar & Basirat (2012) detailed the formulation of the SBFEM to investigate seismic problems. Tohidvand & Hajialilue-Bonab (2014) conducted a seismic soil-structure interaction analysis using the coupled scaled boundary spectral element-spectral element method (SBSE-SEM). They used an adaptive method to calculate acceleration unit impulse matrix in seismic loading condition. Hassanzadeh et al. (2018) proposed the scaled boundary point interpolation method and applied it in modeling seismic soil-tunnel interaction problem.

The coupled PFEM-SBFEM has not yet been used to model seismic wave propagation problems. Application of the polygonal elements to model near field of a domain can enhance mesh generation procedure. In addition, by increasing the number of nodes per element high order shape functions can be achieved. In this paper, the coupled polygonal finite element-scaled boundary finite element method is used to model wave propagation problems, for the first time.

II. The Polygonal Finite Element Method

The main step in the construction of the polygonal elements is the evaluation of shape functions. Wachspress (1975) proposed an easy approach for the definition of shape functions of the polygonal elements. The Wachspress shape functions use the principles of perspective geometries to satisfy the nodal interpolation and linearity on boundaries (Biabanaki et al., 2011). A detailed description of the Wachspress method can be found in Meyer et al. (2002). Here a brief explanation of the approach is presented. Wachspress shape function can be defined using the below expression (Meyer et al., 2002):

$$\phi_i{}^{w} = \frac{w_i(x)}{\sum_{j=1}^{n} w_j(x)} \tag{1}$$

where $w_i(x)$ can be computed as:

$$w_i(x) = \frac{A(p_{i-1}, p, p_{i+1})}{A(p_{i-1}, p_i, p)A(p_i, p_{i+1}, p)} = \frac{\cot\delta_i + \cot\gamma_i}{\left\|x - x_i\right\|^2} \tag{2}$$

A(a,b,c) is the signed area of the predefined triangle (abc) and P_i is the i^{th} node of the polygon and can be defined as shown in Figure 2. The variables γ_i and δ_i are detailed in Figure 2 and should be calculated for each integration point and interpolation node. Vector calculus operations can be employed to determine Wachspress shape functions. By defining vertices of a pre-considered triangle (p_i, p_i+1, p) as (a_1, a_2), (b_1, b_2) and (x_1, x_2), cot δ_i can be obtained by (Meyer et al., 2002):

$$\cot\delta_i = \frac{(b_1 - a_1)(x_1 - a_1) + (b_2 - a_2)(x_2 - a_2)}{(b_1 - a_1)(x_2 - a_2) + (x_1 - a_1)(b_2 - a_2)} \tag{3}$$

Other steps of the polygonal finite element method are so similar to the conventional finite element approach.

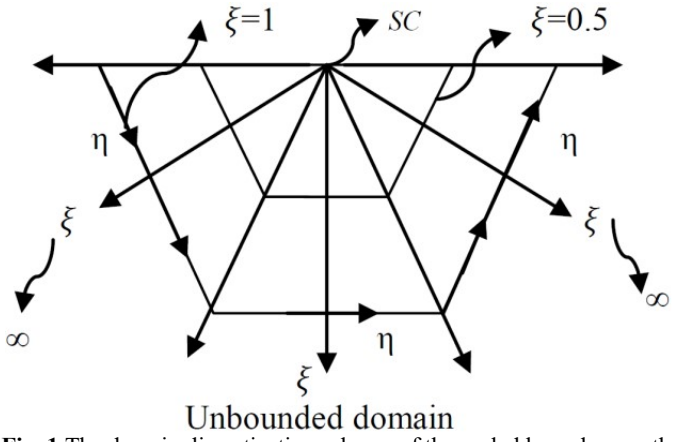

Fig. 1 The domain discretization scheme of the scaled boundary method

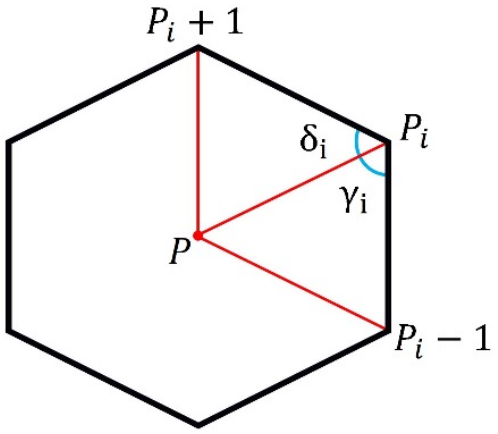

Fig. 2 A sample polygonal element

III. The Scaled Boundary Finite Element Method

The SBFEM is a relatively novel, semi-analytical approach which can be applied to accurately model bounded and unbounded media (Deeks et al., 2002). This method has four coefficient matrices (E_0, E_1, E_2, and M_0) where E_0 is a positive definite, symmetric matrix and can be calculated using Eq. 4. E_1 is a non-symmetric matrix, which contains both shape functions and their derivatives. E_1 can be calculated using Eq. 5. E_2 is another symmetric coefficient matrix and can be derived using Eq. 6. M_0 can be considered as the mass matrix of unbounded medium and Eq. 7, can be used to construct this matrix (Deeks et al., 2002).

$$[E^0] = \int_{-1}^{+1} [B^1]^T [D][B^1] |J| \, d\eta \tag{4}$$

$$[E^1] = \int_{-1}^{+1} [B^2]^T [D][B^1] |J| \, d\eta \tag{5}$$

$$[E^2] = \int_{-1}^{+1} [B^2]^T [D][B^2] |J| \, d\eta \tag{6}$$

$$[M^0] = \int_{-1}^{1} [N(\eta)]^T \rho [N(\eta)] |J| d\eta \tag{7}$$

In these equations, [D] and [ρ] are the elasticity and density matrices respectively, and [B^1] includes shape functions and [B^2] contains derivatives of shape functions (Deeks et al., 2002). For the time-domain modeling of wave propagation in unbounded domains by using the scaled boundary method, a unit impulse response should be calculated. This response can be stated in terms of acceleration, velocity or displacement impulse responses. For homogenous unbounded media, scaled boundary equations for these responses have been derived (Wolf et al., 1996). The dynamic stiffness matrix of an unbounded medium can be computed using Eq. 8. In this Eq., s is the parameter of dimension (s=2 for 2D and s=3 for 3D problems).

In order to analyze unbounded media in the time domain, the scaled boundary equation in acceleration unit impulse response has been derived previously (Wolf et al., 1996). Eq. 9, presents the integration formula to calculate the acceleration unit impulse response matrix.

$$\begin{aligned} &([S^\infty(\omega)] + [E^1])[E^0]^{-1}([S^\infty(\omega)] + [E^1]^T) \\ &-(s-2)[S^\infty(\omega)] - \omega [S^\infty(\omega)]_{,\omega} \\ &-[E^2] + \omega^2 [M^0] = 0 \end{aligned} \tag{8}$$

$$\begin{aligned} &\int_0^t [M^\infty(t-\tau)][E^0]^{-1}[M^\infty(\tau)] d\tau + t\int_0^t [M^\infty(\tau)] d\tau + \\ &([E^1][E^0]^{-1} - (0.5(s+1))[I]) \int_0^t \int_0^\tau [M^\infty(\tau')] d\tau' d\tau + \\ &\int_0^t \int_0^\tau [M^\infty(\tau')] d\tau' d\tau ([E^0]^{-1}[E^1]^T - (0.5(s+1))[I]) - \\ &\frac{t^3}{6}([E^2] - [E^1][E^0]^{-1}[E^1]^T) H(t) - t[M^0] H(t) = 0 \end{aligned} \tag{9}$$

Where *H(t)* is the Heaviside-step function. After computing the acceleration unit impulse response matrix, the equation of motion can be constructed. For dynamic or seismic loading cases, this equation can be written as:

$$\begin{aligned} &\begin{bmatrix} k_{ii} & k_{i\Gamma} \\ k_{\Gamma i} & k_{\Gamma\Gamma} \end{bmatrix} \begin{bmatrix} u_i(t) \\ u_\Gamma(t) \end{bmatrix} + \begin{bmatrix} C_{ii} & C_{i\Gamma} \\ C_{\Gamma i} & C_{\Gamma\Gamma} \end{bmatrix} \begin{bmatrix} v_i(t) \\ v_\Gamma(t) \end{bmatrix} + \\ &\begin{bmatrix} M_{ii} & M_{i\Gamma} \\ M_{\Gamma i} & M_{\Gamma\Gamma} + \gamma \Delta t M_0^\infty \end{bmatrix} \begin{bmatrix} a_i(t) \\ a_\Gamma(t) \end{bmatrix} = \begin{bmatrix} p_i(t) \\ p_\Gamma(t) - r_\Gamma(t) \end{bmatrix} \end{aligned} \tag{10}$$

Where [M], [C] and [K] are the mass, damping and stiffness matrices, respectively and {a}, {v} and {u} are the acceleration, velocity and displacement vectors. The subscript Γ indicates degrees of freedom of the nodes on the near and far field interface. The subscript (i) denotes degrees of freedom on the remaining nodes of the structure. In this equation, {r_Γ} is the interaction force vector, and for a seismic loading case can be calculated as:

$$r(t) = \int_0^t M^\infty(t-\tau)\{a(\tau) - a_g(\tau)\} d\tau \tag{11}$$

Where $M^\infty(t)$ is the acceleration unit impulse response matrix and ag is the seismic input acceleration.

IV. Numerical Verifications

In this section, two numerical benchmark examples are investigated to show the accuracy and efficiency of the proposed polygonal finite element-scaled boundary finite element method to analyze soil structure interaction problems.

A. An Elastic Half-Space Subjected to the Ricker Wavelet Type Dynamic Load

In this example, an elastic half-space is undertaken to illustrate the capability of the PFE-SBFEM to model wave propagation problems. The elastic half space on the Cartesian

coordinate system is shown in Figure 3(a). This half-space has an elastic modulus as E=2.66×10 kN/m^2, Poisson's ratio as v=0.33 and a mass density ρ=2×10^3 kg/m^3. Figure 3(a) also shows the details of the loading and the observation points. Figure 3(b) shows the used polygonal mesh to discretize the assumed near field soil domain, and Figure 3(c) shows the Ricker wavelet type dynamic load which is applied to the domain horizontally. To model the bounded medium, the polygonal finite element method is used. The radiation damping effect of the unbounded soil medium is modeled by the scaled boundary approach. The results of the coupled boundary element-finite element (BE-FE) method extracted from (Lehmann, 2005) are used to verify the achieved results. The result of the calculated horizontal displacement of point A is shown for both above-mentioned approaches in Figure 4. It is shown that there is an excellent agreement between the coupled PFE-SBFEM and BE-FE approaches.

B. An Elastic Half-Space Subjected to a Strip Dynamic Load

An elastic soil medium subjected to a vertical strip dynamic load is assumed in this example. The considered medium and the applied dynamic load are detailed in Figure 5(a). The polygonal finite element mesh which is used to discretize the near-field soil domain is shown in Figure 5(b). The considered half-space has elastic modulus E=1.77×10^7 kN/m^2 and shear wave velocity equal to 4.74×10^2 m/s. The load intensity is equal to 68980 kN/m. The results of the proposed PFE-SBFEM are compared with the results of the boundary element method extracted from (Estorff et al., 2000). The comparison of the results is shown in Figure 5(c). It is shown that an excellent agreement between the two methods is achieved.

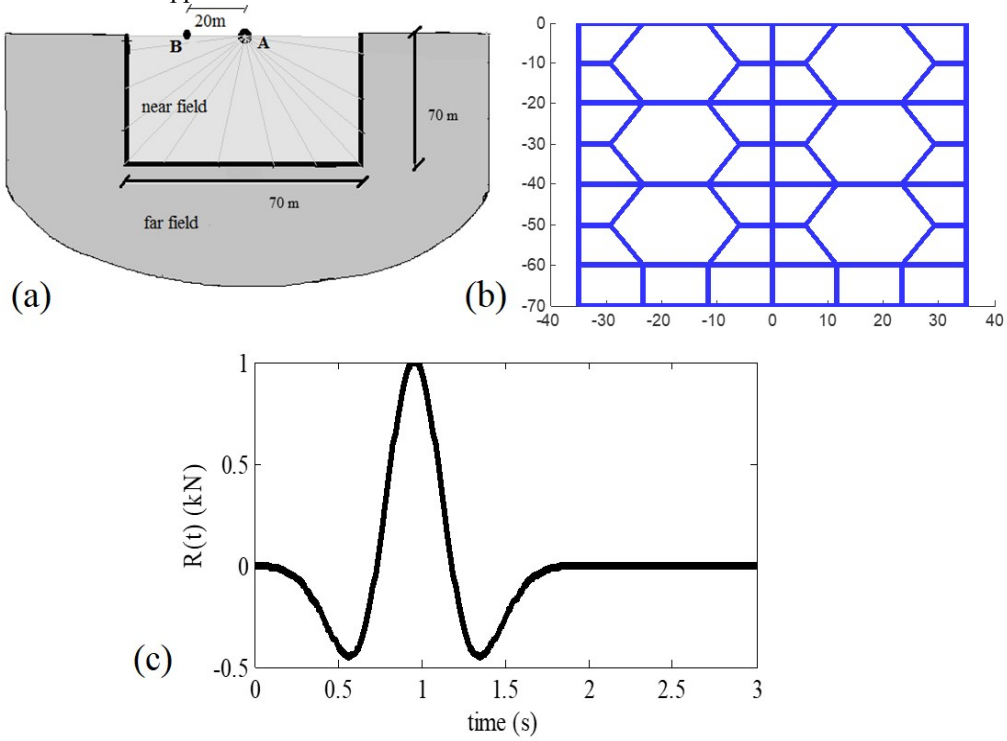

Fig. 3 The assumed elastic half-space (b) The used polygonal elements in the near field (c) Time history of the load function

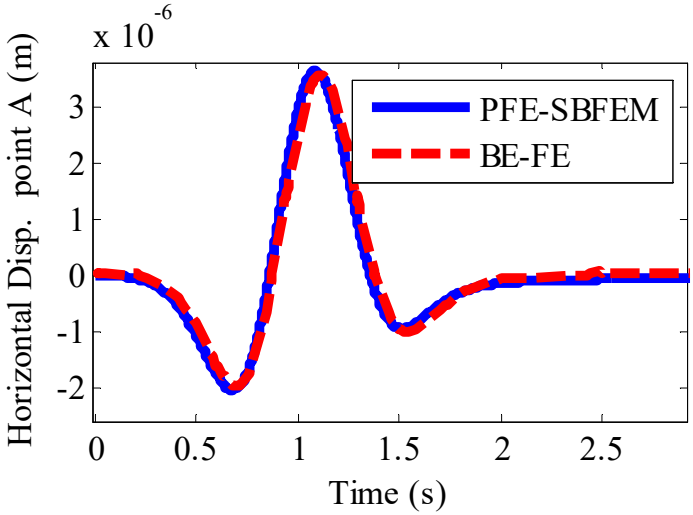

Fig. 4 The horizontal displacement time histories of the point A

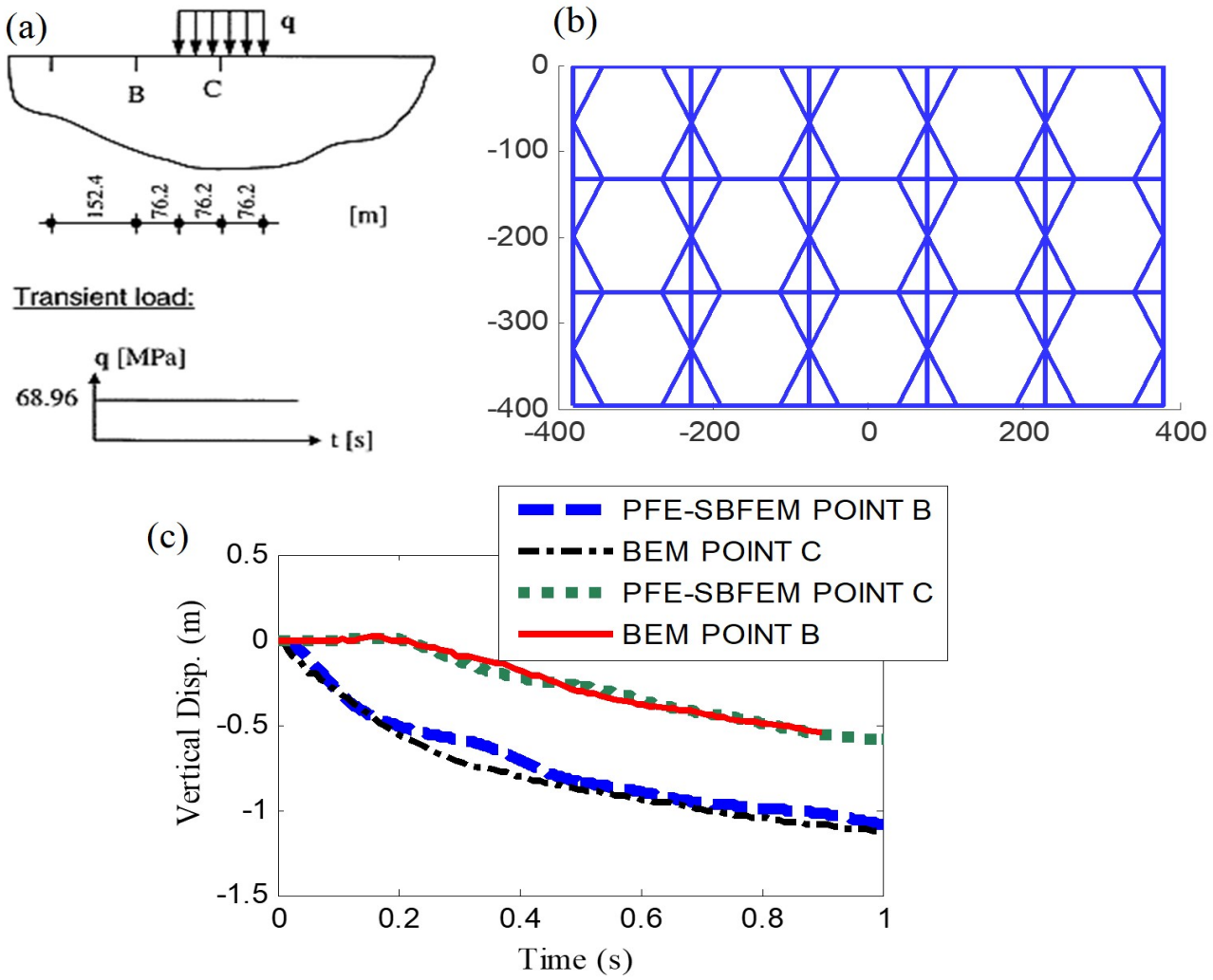

Fig. 5 (a) The considered near field soil medium and the applied load time history. (b) The used polygonal finite element meshes (c) Displacement time histories of the points B and C.

V. Numerical and Experimental Studies

As a global issue, the overgrowth of the population in large cities has led to a serious scarcity of proper above-ground space for conveying of traffic and subsequently urges the use of underground space. Construction and development of underground transportation lines like metro tunnels in urban areas is an effective alternative to reduce the volume of traffic. Evaluation of these tunnels against seismic excitations is one of the fundamental steps in the design process of such facilities. Therefore, seismic tunnel response analyses have attracted increasing attention in recent years. In this section, circular and rectangular tunnels are selected to experimentally model the seismic behavior of tunnels using a 1g shaking table test. Then, the achieved results are used for verifying the proposed PFE-SBFE approach.

A. Circular Tunnels

To experimentally model the seismic behavior of tunnels and verify the proposed polygonal finite element-scaled boundary finite element method, a shaking table test was designed. Figure 6 shows the shaking table apparatus, and the shear box used for this test. The soil container used in the study is a laminar shear box with overall dimensions of 1.32 m length (x), 0.86 m width (y) and 0.82 m height (z). The soil container was constructed by 21 steel frames stacked on each other. A circular tunnel with rigid lining is considered. To model rigid lining, an aluminum box with a high elastic modulus is used (Figure 7).

Prior to the loading procedure with the shaking table, a hammer blow test was performed manually on the soil column. The soil was poured inside the shear box on the shaking table using the automatic pluviation device by placing a vertical array of some accelerometers within the soil. A plastic hammer was then used to create excitation in the first accelerometer placed at the top of the soil column. The difference between arrival times of shear waves to each accelerometer was measured. The shear wave velocity of the soil within the shear box was obtained in intervals between the accelerometers with distance to time ratios. As a result, the material properties of the surrounding soil in the model are defined by the shear wave velocity vs=80 m/s, Poisson's ratio v=0.3, and mass density ρ=1.55 ton/m3. Table 1 shows the values of the material properties for the soil used in the experimental model.

As the scaled boundary method can model the radiation damping effect of the semi-infinite soil medium, only a small part of the soil domain is modeled. In addition, because of the symmetry, only half of the system is modeled. Figure 8 shows the geometry of the system which is used in numerical study. The model is subjected to some periodic base excitations. The acceleration time history of the first applied vibration is shown in Figure 9. The time history of horizontal acceleration of point A is shown in Figure 10. Excellent agreement can be observed between the results of the experimental test and the PFE-SBFEM. For the second case, another acceleration time history is applied to the shaking table apparatus. The time history of the applied acceleration is shown in Figure 11. The acceleration time history resulting from the second test is shown in Figure 12. As can be clearly seen, the results of PFE-SBFEM are perfectly consistent with the experimental data.

B. Rectangular Tunnels

A shaking table test of a rectangular tunnel is designed to further investigate the accuracy of the proposed polygonal finite element-scaled boundary finite element method. Like the previous test, the rigid lining is considered for the tunnel. Figure 13 displays the used aluminum box in the shaking table test. Shear wave velocity of the soil in the used model is evaluated by a hammer blow test same as the first modeling and mass density of the soil is determined directly from the constructed model. The material properties of the surrounding soil in the model are defined by the shear wave velocity v_s=50 m/s, v=0.3, and mass density ρ=1.55 ton/m^3. Table 2 shows the values of material properties for the considered model.

The geometry of the system used in the numerical modeling is detailed in Figure 14(a), and the generated polygonal mesh can be seen in Figure 14(b). Like the circular tunnel case, two different input acceleration time histories are applied in this test. The first applied acceleration time history is shown in Figure 15. The horizontal acceleration of point A is shown in Figure 16. It is clearly shown that the result of the shaking table test is almost matched with those of the coupled polygonal finite element-scaled boundary finite element method. The second input acceleration time history is illustrated in Figure 17. The acceleration time histories obtained from the experimental and the numerical studies are shown in Figure 18. As it is shown, the result of the employed numerical approach perfectly concurs with the experimental data.

Table 1 The soil properties used in the first experiment

Material property	Value
Mass density (ton/m^3)	1.55
Shear wave velocity (m/s)	80

Table 2 The soil properties used in the second experiment

Material property	Value
Mass density (ton/m^3)	1.55
Shear wave velocity (m/s)	50

Fig. 6 The shaking table apparatus and the used laminar shear box in experiments

Fig. 7 The used aluminum box to model lining of the circular tunnel

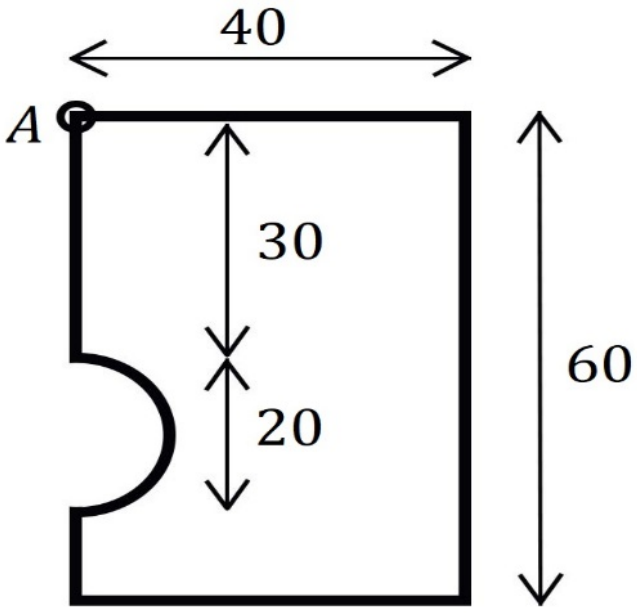

Fig. 8 The geometry of the system comprising of the circular tunnel and the surrounding soil medium

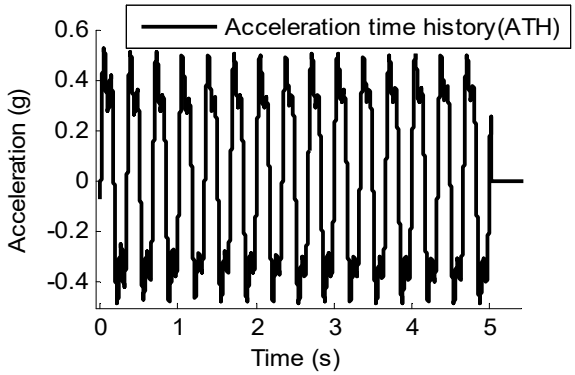

Fig. 9 Acceleration time history of the applied vibration in the shaking table test for the first analysis

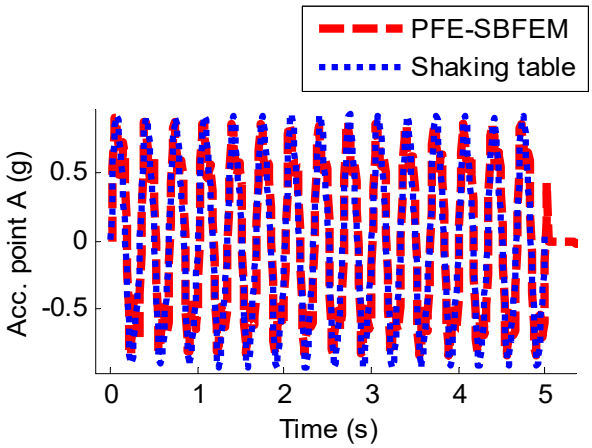

Fig. 10 The horizontal acceleration of point A.

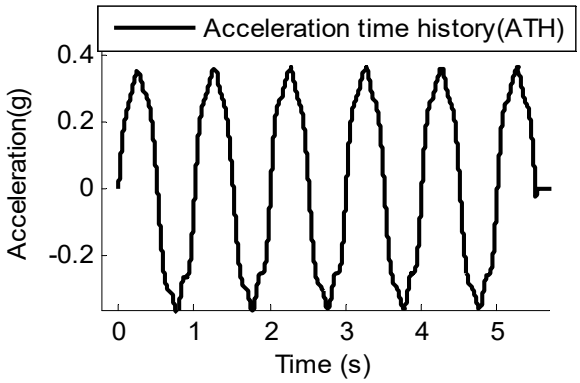

Fig. 11 The acceleration time history of the applied vibration in the shaking table test for the second test

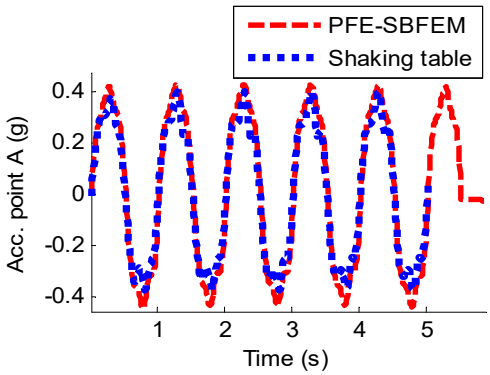

Fig. 12 The horizontal acceleration of point A.

Fig. 13 The aluminum box used as the lining of the tunnel in the second shaking table test

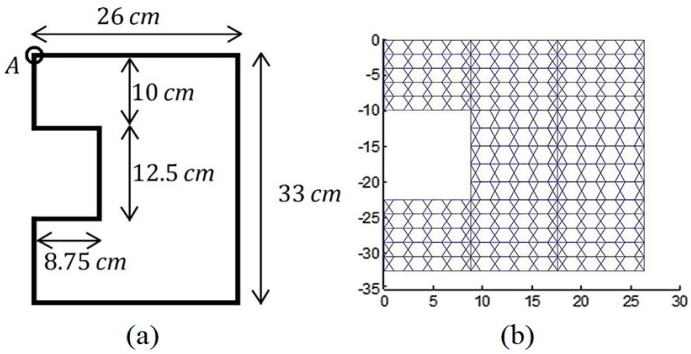

Fig. 14 The geometry of the system comprising of a rectangular tunnel and the surrounding soil which is used in the second shaking table test. (b) The used polygonal mesh

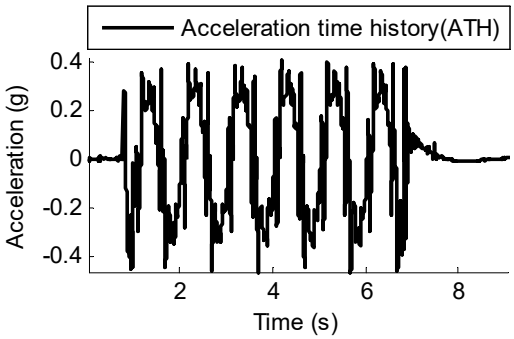

Fig. 15 The input acceleration time history

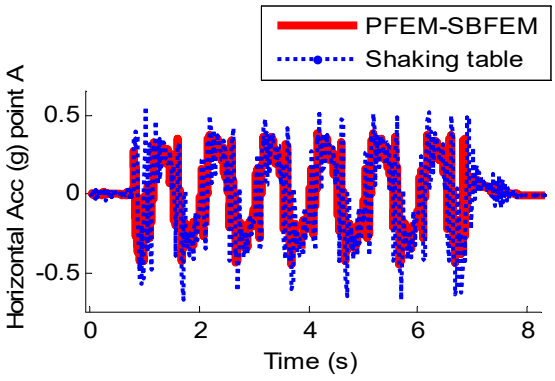

Fig. 16 The acceleration time history of point A

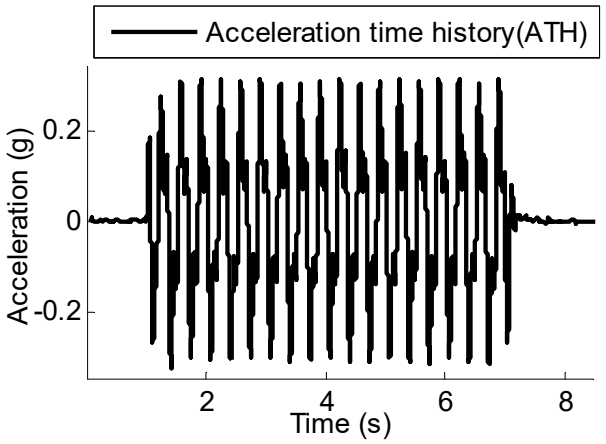

Fig. 17 The input acceleration time history

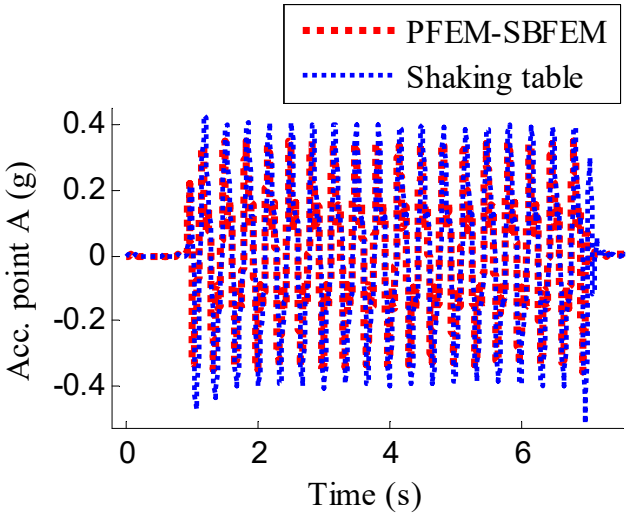

Fig. 18 The acceleration time history of point A

VI. CONCLUSION

In this paper, a coupled polygonal finite element-scaled boundary finite element method was presented for the seismic evaluation of soil-tunnel interaction analysis. The use of the polygonal elements makes the mesh generation procedure considerably easier than corresponding procedure with the conventional elements. In addition, by using more nodes per element in the polygons, p-refinement can be done, and better interpolation can be achieved. Application of the presented coupled PFE-SBFEM was investigated using two numerical benchmark examples. Excellent agreement was observed between the results of the PFE-SBFEM and the other numerical approaches (like the conventional boundary element method). After these verifications, two shaking table tests were used for modeling the seismic behavior of circular and rectangular tunnels. The results of the PFE-SBFEM were compared with those of shaking table tests and excellent agreement between them was obtained. It can be concluded that the proposed coupled method can model the seismic response of tunnels efficiently and with a high accuracy.

ACKNOWLEDGMENT

We extend our thanks to the reviewers for their meticulous attention to detail and constructive suggestions that greatly improved the quality of this manuscript. Your contributions have been instrumental in shaping this work.

AUTHORS' CONTRIBUTIONS

Vida Nikvand conducted the main data analysis, contributed to the data collection, preprocessing, and interpretation, and was responsible for drafting the initial manuscript. Masoud Hajialilue Bonab assisted in the development of the methodology and performed validation checks, provided supervision, conceptual guidance, and critical revision of the manuscript. All authors read and approved the final manuscript.

CONFLICT OF INTEREST

The authors have not disclosed any competing interests.

OPEN ACCESS

REFERENCES

Bazyar M.H., Basirat B. (2012). Dynamic Soil-Structure Interaction Analysis under Seismic Loads Using the Scaled Boundary Finite-Element Method. *Journal of Seismology and Earthquake Engineering*, 14(1), 57-68.

Bazyar M.H., Talebi A. (2015). Transient seepage analysis in zoned anisotropic soils based on the scaled boundary finite-element method. *International Journal for Numerical and Analytical Methods in Geomechanics*, 39(1), 1-22. https://doi.org/10.1002/nag.2291.

Berenger J.P. (1994). A perfectly matched layer for the absorption of electromagnetic waves. *Journal of Computational Physics*, 114(2), 185-200. https://doi.org/10.1006/jcph.1994.1159.

Biabanaki S.O.R., Khoei A.R. (2012). A polygonal finite element method for modeling arbitrary interfaces in large deformation problems. *Computational Mechanics*, 50(1), 19-33. https://doi.org/10.1007/s00466-011-0668-4.

Binesh S.M., Raei S. (2014). Upper bound limit analysis of cohesive soils using mesh-free method. *Geomechanics and Geoengineering*, 9(4), 265-278. https://doi.org/10.1080/17486025.2014.887229.

Bretas E.M., Lemos J.V., Lourenço P.B. (2016). Seismic analysis of masonry gravity dams using the discrete element method: implementation and application. *Journal of Earthquake Engineering*, 20(2), 157-184. https://doi.org/10.1080/13632469.2015.1085463.

Celebi E., Göktepe F., Karahan N. (2012). Non-linear finite element analysis for prediction of seismic response of buildings considering soil-structure interaction. *Natural Hazards and Earth System Sciences*, 12(11), 3495-3505. https://doi.org/10.5194/nhess-12-3495-2012.

Chen Y.C.S., Rashed Y.F., Golberg M.A. (1998). A mesh-free method for linear diffusion equations. *Numerical Heat Transfer-Part B*, 33(4), 469-486. https://doi.org/10.1080/10407799808915044.

Chew W.C., Liu Q.H. (1996). Perfectly matched layers for elastodynamics: a new absorbing boundary condition. *Journal of Computational Acoustics*, 4(4), 341-359. https://doi.org/10.1142/S0218396X96000118.

Chi H., Talischi C., Lopez-Pamies O., Paulino G.H. (2015). Polygonal finite elements for finite elasticity. *International Journal for Numerical Methods in Engineering*, 101(4), 305-328. https://doi.org/10.1002/nme.4802.

Deeks A.J., Wolf J.P. (2002). A virtual work derivation of the scaled boundary finite-element method for elastostatics. *Computational Mechanics*, 28(6), 489-504. https://doi.org/10.1007/s00466-002-0314-2.

Duan W., Kirby R., Mudge P., Gan T.H. (2016). A one dimensional numerical approach for computing the eigenmodes of elastic waves in buried pipelines. *Journal of Sound and Vibration*, 384, 177-193. https://doi.org/10.1016/j.jsv.2016.08.013.

Fontara I.K., Schepers W., Savidis S., Rackwitza F. (2017). FE/PML numerical schemes for dynamic soil-structure interaction and seismic wave propagation analysis. *Procedia Engineering*, 199, 2348-2353. https://doi.org/10.1016/j.proeng.2017.09.222.

Genes M.C., Kocak S. (2002). Seismic Analyses of Soil Structure Interaction Systems by Coupling the Finite Element and the Scaled Boundary Finite Element Methods. In: *Proceedings of the ECA2002 International Symposium on Structural and Earthquake Engineering*, Middle East Technical University, ankara, Turkey.

Grigoriev M.M., Dargush G.F. (2004a). Efficiency and accuracy of higher-order boundary-element methods for steady convective heat diffusion. *Numerical Heat Transfer, Part B: Fundamentals*, 45(2), 109-133. https://doi.org/10.1080/10407790490253874.

Grigoriev M.M., Dargush G.F. (2004b). A multilevel boundary-element method for two-dimensional steady heat diffusion. *Numerical Heat Transfer, Part B: Fundamentals*, 46(4), 329-356. https://doi.org/10.1080/10407790490475346.

Hajialilue-Bonab M., Balazadeh B., Tohidvand H.R. (2015). The scaled boundary spectral element method for dynamics of unbounded media with nonhomogeneity in radial direction. *Asian Journal of Civil Engineering*. 16, 81-96.

Hajialilue-Bonab M., Razavi S.K. (2015). A study of soil-nailed wall behavior at limit states. *Proceedings of the Institution of Civil Engineers-Ground Improvement*, 169(1), 64-76. https://doi.org/10.1680/jgrim.14.00021.

Hajialilue-Bonab M., Tohidvand H.R. (2015). A modified scaled boundary approach in frequency domain with diagonal coefficient matrices. *Engineering Analysis with Boundary Elements*, 50, 8-18. https://doi.org/10.1016/j.enganabound.2014.07.001.

Hassanzadeh M., Tohidvand H.R., Hajialilue-Bonab M., Javadi A.A. (2018). Scaled boundary point interpolation method for seismic soil-tunnel interaction analysis. *Computers and Geotechnics*, 101, 208-216. https://doi.org/10.1016/j.compgeo.2018.05.007.

Junyi Y., Feng J., Yanjie X., Guanglun W., Chuhan Z. (2003). A seismic free field input model for FE-SBFE coupling in time domain. *Earthquake Engineering and Engineering Vibration*, 2(1), 51-58. https://doi.org/10.1007/BF02857538.

Lehmann L. (2005). An effective finite element approach for soil-structure analysis in the time-domain. *Structural Engineering and Mechanics*, 21(4), 437-450. https://doi.org/10.12989/sem.2005.21.4.437.

Lin G., Zhang Y., Hu Z., Zhong H. (2014). Scaled boundary isogeometric analysis for 2D elastostatics. *Science China Physics, Mechanics and Astronomy*, 57(2), 286-300. https://doi.org/10.1007/s11433-013-5146-x.

Meyer M., Barr A., Lee H., Desbrun M. (2002). Generalized barycentric coordinates on irregular polygons. *Journal of Graphics Tools*, 7(1), 13-22. https://doi.org/10.1080/10867651.2002.10487551.

Nath U.K., Hazarika P.J. (2013). Parametric study of pile cap lateral resistance: finite element analysis. *International Journal of Geotechnical Engineering*, 7(3), 273-281. https://doi.org/10.1179/1938636213Z.00000000039.

Nguyen-Xuan H. (2017b). A polytree-based adaptive polygonal finite element method for topology optimization. *International Journal for Numerical Methods in Engineering*, 110(10), 972-1000. https://doi.org/10.1016/j.cma.2017.07.035.

Nguyen-Xuan H. (2017c). A polygonal finite element method for plate analysis. *Computers and Structures*, 188, 45-62. https://doi.org/10.1016/j.compstruc.2017.04.002.

Nguyen-Xuan H., Nguyen-Hoang S., Rabczuk T., Hackl K. (2017a). A polytree-based adaptive approach to limit analysis of cracked structures. *Computer Methods in Applied Mechanics and Engineering*, 313, 1006-1039. https://doi.org/10.1016/j.cma.2016.09.016.

Pak R.Y.S., Guzina B.B. (1999). Seismic soil-structure interaction analysis by direct boundary element methods. *International Journal of Solids and Structures*, 36(31-32), 4743-4766. https://doi.org/10.1016/S0020-7683(98)00263-7.

Rafiezadeh K., Ataie-Ashtiani B. (2014). Transient free-surface seepage in three-dimensional general anisotropic media by BEM. *Engineering Analysis with Boundary Elements*, 46, 51-66. https://doi.org/10.1016/j.enganabound.2014.04.025.

Rajagopal A., Kraus M., Steinmann P. (2018). Hyperelastic analysis based on a polygonal finite element method. *Mechanics of Advanced Materials and Structures*, 25(11), 930-942. https://doi.org/10.1080/15376494.2017.1329463.

Razavi S.K., Hajialilue Bonab M. (2017). Study of soil nailed wall under service loading condition. *Proceedings of the Institution of Civil Engineers-Geotechnical Engineering*, 170(2), 161-174. https://doi.org/10.1680/jgeen.16.00006.

Ribeiro D.B., de Paiva J.B. (2014). A new BE formulation coupled to the FEM for simulating vertical pile groups. *Engineering Analysis with Boundary Elements*, 41, 1-9. https://doi.org/10.1016/j.enganabound.2014.01.007.

Seiphoori A., Haeri S.M., Karimi M. (2011). Three-dimensional nonlinear seismic analysis of concrete faced rockfill dams subjected to scattered P, SV, and SH waves considering the dam–foundation interaction effects. *Soil Dynamics and Earthquake Engineering*, 31(5-6), 792-804. https://doi.org/10.1016/j.soildyn.2011.01.003.

Sukumar N., Tabarraei A. (2004). Conforming polygonal finite elements. *International Journal for Numerical Methods in Engineering*, 61(12), 2045-2066. https://doi.org/10.1002/nme.1141.

Tabarraei A., Sukumar N. (2006). Application of polygonal finite elements in linear elasticity. *International Journal of Computational Methods*, 3(04), 503-520. https://doi.org/10.1142/S021987620600117X.

Talischi C., Pereira A., Paulino G.H., Menezes I.F., Carvalho M.S. (2014). Polygonal finite elements for incompressible fluid flow. *International Journal for Numerical Methods in Fluids*, 74(2), 134-151. https://doi.org/10.1002/fld.3843.

Tohidvand H.R., Hajialilue-Bonab M. (2014). Seismic soil structure interaction analysis using an effective scaled boundary spectral element approach. *Asian Journal of Civil Engineering*. 15(4), 501-516.

Von Estorff O., Firuziaan M. (2000). *Engineering Analysis with Boundary Elements*, 24(10), 715-725. https://doi.org/10.1016/S0955-7997(00)00054-0.

Wachspress E.L. (1975). A *rational finite element basis*. Elsevier press, Amsterdam, Netherlands.

Wolf J.P., Song C. (1996). *Finite-element modelling of unbounded media*. Wiley, Chichester, England, UK.

Xu L., Ye J. (2019). DEM algorithm for progressive collapse simulation of single-layer reticulated domes under multi-support excitation. *Journal of Earthquake Engineering*, 23(1), 18-45. https://doi.org/10.1080/13632469.2017.1309606.

Yang Y.B., Hung H.H. (1997). A parametric study of wave barriers for reduction of train-induced vibrations. *International Journal for Numerical Methods in Engineering*, 40(20), 3729-3747. https://doi.org/10.1002/(SICI)1097-0207(19971030)40:20<3729::AID-NME236>3.0.CO;2-8.

Yang Y.B., Hung H.H., Chang D.W. (2003). Train-induced wave propagation in layered soils using finite/infinite element simulation. *Soil Dynamics and Earthquake Engineering*, 23(4), 263-278. https://doi.org/10.1016/S0267-7261(03)00003-4.

Yeong-bin Y., Hsiao-hui H. (2009). Wave propagation for train-induced vibrations: a finite/infinite element approach. World scientific, https://doi.org/10.1142/7062.

Zhou M.X., Wang J.T., Jin F., Gui Y., Zhu F. (2014). Real-Time Dynamic Hybrid Testing Coupling Finite Element and Shaking Table. *Journal of Earthquake Engineering*, 18(4), 637-653. https://doi.org/10.1080/13632469.2014.897276.